

Vertical and temporal distribution of insolation in gaps in an old-growth coniferous forest

Stuart B. Weiss

Abstract: The combination of canopy access at the Wind River Canopy Crane Research Facility, hemispherical photography, and long-term insolation data provided estimates of vertical and temporal distributions of insolation in nine canopy gaps in a 65 m tall Douglas-fir (*Pseudotsuga menziesii* (Mirb.) Franco) – western hemlock (*Tsuga heterophylla* (Raf.) Sarg.) forest. Yearly insolation (long-term data from Portland, Oreg.) exhibited a sigmoidal pattern with height, with a bright zone (>4200 MJ/m²) above 50 m, a transition zone from 45 to 30 m (2000 MJ/m²), and less rapid decrease from 30 to below 10 m (600 MJ/m²). Intergap variation peaked between 20 and 40 m. Interannual variation of yearly insolation (CV = SD/mean) was about 5% throughout the canopy. Seasonality of insolation was driven by solar angle and cloudiness. Diffuse insolation was 50% of annual above-canopy flux, increasing to nearly 70% at 1.5 m, and diffuse proportion was greater in winter and spring. Hourly simulations under clear and cloudy conditions provided an appropriate time scale for modeling photosynthesis. Estimated leaf area index peaked at 30–35 and 5–10 m but was underestimated (3.7 vs. 9.1 m²/m² from direct measurements) because of foliage clumping. The methods documented highly variable distributions of insolation driven by forest structure, cloudiness, and seasonal changes in solar angle.

Résumé : La combinaison de l'accès à la canopée au Wind River Canopy Crane Research Facility, de la photographie hémisphérique et de données d'insolation à long terme a permis d'estimer les distributions verticale et horizontale de l'insolation dans neuf ouvertures de la canopée d'une forêt de douglas de Menzies (*Pseudotsuga menziesii* (Mirb.) Franco) et de pruche de l'Ouest (*Tsuga heterophylla* (Raf.) Sarg.) de 65 m de hauteur. L'insolation annuelle (données à long terme de Portland en Oregon) présente avec la hauteur un patron sigmoïde, avec une zone brillante (>4200 MJ/m²) au-dessus de 50 m, une zone de transition entre 45 et 30 m (2000 MJ/m²) et une diminution moins rapide de 30 m à moins de 10 m (600 MJ/m²). La pointe de la variation entre les ouvertures se situait entre 20 et 40 m. La variation inter-annuelle de l'insolation annuelle (CV = e.t./moyenne) était d'environ 5% à travers la canopée. La variation saisonnière de l'insolation était contrôlée par l'angle d'élévation du soleil et la nébulosité. L'insolation diffuse qui constituait 50% du flux annuel au-dessus de la canopée, augmentait à près de 70% à 1,5 m et la proportion d'insolation diffuse était plus élevée en hiver qu'au printemps. Les simulations horaires sous conditions claires et nuageuses fournissent un pas de temps approprié pour modéliser la photosynthèse. L'indice de surface foliaire estimé (LAI) atteignait des pointes à 30–35 m et à 5–10 m, mais était sous-estimé (3,7 versus 9,1 m²/m² mesuré directement) à cause du feuillage qui formait des touffes. Les méthodes ont révélé des distributions hautement variables de l'insolation dues à la structure de la forêt, à la nébulosité et au changement saisonnier de l'angle d'élévation du soleil.

[Traduit par la Rédaction]

Introduction

Quantitative estimates of the spatial and temporal distribution of shortwave insolation in forests are important, because insolation is the only source of photosynthetically active radiation (PAR) and the dominant input to the surface energy balance (Geiger 1965). Forest canopies at a point in time are complex three-dimensional structures that intercept, transmit, and reflect insolation (Parker 1995), producing steep vertical gradients and horizontal variation from gaps into closed sites. Seasonal phenology and longer scale changes in structure add a fourth dimension to canopy structure (Margolis et al. 1995). The time course of global insolation (direct +

diffuse above the canopy) adds yet more dimensionality to the distribution of insolation within a forest. Potential clear-sky insolation varies deterministically with daily and seasonal solar angle, and vertical penetration into canopies depends strongly on solar angle. Cloud cover reduces total insolation, changes fractions of direct and diffuse insolation, and varies seasonally and interannually. All of these factors contribute to a highly dynamic multidimensional (three spatial and one temporal) insolation environment. The insolation environment in turn drives basic ecosystem functions such as productivity and evapotranspiration, and the pattern of forest growth responds to and further changes the distribution of insolation. Quantitative descriptions of the distributions of insolation at different temporal and spatial scales are an important step in understanding the structure and function of forested ecosystems.

Quantifying both the spatial and the temporal variability of insolation in forests is a challenge. Moving sensors can only provide spot measurements over short time periods and can be difficult to integrate through time because of hourly

Received June 23, 1999. Accepted August 14, 2000.
Published on the NRC Research Press website on
November 30, 2000.

S.B. Weiss. Creekside Center for Earth Observations. 27
Bishop Lane, Menlo Park, CA 94025, U.S.A. e-mail:
stbweiss@netscape.net

and monthly changes in solar angle and cloudiness (Parker 1995, 1997; Gendron et al. 1998). Fine-scale temporal structure of insolation can be quantified with stationary sensors, but extensive spatial coverage requires prohibitive numbers of sensors (Reifsnnyder et al. 1972). Hemispherical photography is a well-developed technique for studying forest canopy structure and insolation (Rich 1990). It overcomes temporal limitations, because insolation penetration over an entire year can be estimated from a single photograph in the absence of major seasonal changes in canopy structure. Estimates from hemispherical photographs correlate strongly with measured light (Gendron et al. 1998; Rich et al. 1993; Whitmore et al. 1993). When insolation data are available, hemispherical photographs can estimate absolute insolation fluxes, rather than fluxes relative to open conditions (Rich et al. 1993). It overcomes spatial limitations because numerous sites can be sampled in a relatively short time and photographs can be analyzed later. The photographs themselves provide a permanent record of canopy conditions.

Study of vertical insolation gradients has been difficult without reliable three-dimensional canopy access (Moffett and Lowman 1995). Full vertical characterization has been done only in relatively short forests (Lerdau et al. 1992). Several studies have quantified fine-scale horizontal variation along the forest floor (Becker and Smith 1990; Clark et al. 1996; Nicotra et al. 1999; Thrichon et al. 1998), with some attempts at sampling higher in the canopy with ladders (Clark et al. 1996). Combined with the vertical access provided by a canopy crane and long-term insolation data, hemispherical photography can provide a more complete quantitative description of the spatial and temporal distribution of insolation in a forest.

This work at the Wind River Canopy Crane Research Facility has two objectives: (i) to characterize the architecture of the canopy as seen from canopy gaps, including vertical and horizontal variability in direct and diffuse light penetration and leaf area index (LAI) and (ii) to characterize spatial and temporal variability in light regimes using a particular insolation record, including temporal variability at interannual, monthly, and hourly time scales, and variable fractions of direct and diffuse insolation.

Methods

This research was performed at the Wind River Canopy Crane Research Facility (WRCCRF) in southern Washington State, U.S.A., a cooperative program with the University of Washington, the USDA Forest Service Pacific Northwest Research Station, and the Gifford Pinchot National Forest Wind River District. The WRCCRF consists of a 75 m tall construction tower crane installed in a 500-year-old Douglas-fir (*Pseudotsuga menziesii* (Mirb.) Franco) – western hemlock (*Tsuga heterophylla* (Raf.) Sarg.) forest in the T.T. Munger Research Natural Area, Wind River Experimental Forest in the Cascade Mountains of southern Washington State, U.S.A. (45°49'13.76" N, 121°57'06.88" W, elevation 355 m). The site has a temperate winter-wet, summer-dry climate with 2528 mm of annual precipitation, less than 10% occurring between June and September. Average annual snowfall is 2330 mm, and mean annual temperature is 8.7°C. The tallest tree is 65 m tall. Douglas-fir dominates the upper canopy above 45 m. A dense subcanopy of western hemlocks dominates the middle story along with western redcedars (*Thuja plicata* D. Don) in moister sites. The understory contains many western hemlocks, Pacific silver fir

(*Abies amabilis* (Dougl.) Forbes), Pacific yew (*Taxus brevifolia* Nutt.), and vine maple (*Acer circinatum* Pursh.). For further detailed site descriptions, see Holden (1995) and information published at <http://depts.washington.edu/wrccrf/>.

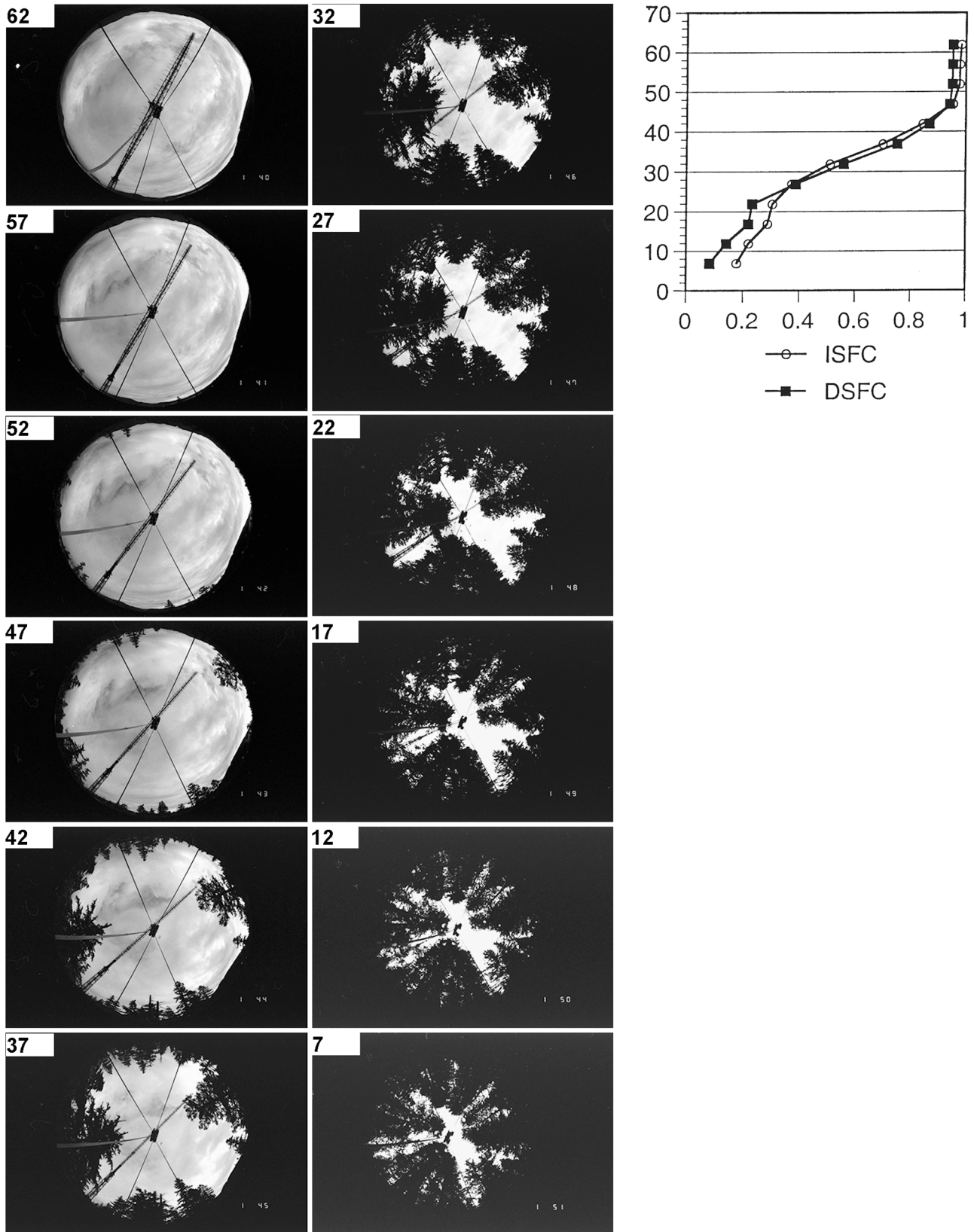
I sampled nine vertical transects in the centers of canopy gaps by taking a hemispherical photograph at 5-m height intervals. Because I sampled centers of gaps, the results represent insolation in well-lit portions of the forest that correspond to the most active outer canopy layer. Digital analysis of photographs estimated penetration of direct and diffuse insolation, which I then combined with long-term insolation data from Portland, Oreg., to estimate mean yearly and mean monthly insolation for each photograph. My analyses included (i) vertical profiles of mean yearly insolation averaged over all nine gaps (gap averaged); (ii) intergap variability in mean yearly insolation; (iii) interannual variability in gap-averaged yearly insolation; (iv) vertical profiles of mean monthly gap-averaged insolation; (v) vertical profiles of monthly fractions of direct and diffuse insolation; (vi) vertical profiles of interannual variability of monthly gap-averaged insolation; (vii) vertical profiles of hourly insolation with height for the winter solstice, spring equinox, and summer solstice on very clear and completely cloudy days; and (viii) vertical profiles of LAI, leaf angle, and clumping estimated from inversion of the Beer–Lambert law (Chen et al. 1991; Rich et al. 1995).

Hemispherical photographs were taken with standard procedures (Rich 1989, 1990), using Kodak TriX PAN 400 ASA black and white film with a Nikkor 8-mm lens and Nikon FM1 camera body mounted on a self-leveling platform (gimbals) attached to a monopod. A red filter was used to enhance contrast between foliage and sky, unless light levels were extremely low deep in the canopy. The gondola was positioned above a gap, and a photograph was taken every 5 m as the gondola descended. Following a light reading, the shutter speed, F-stop, and filter were adjusted. The camera assembly was then lifted so that the lens was just above the gondola frame. A self-timer allowed the camera to steady at a level position, and an exposure was taken. Crane azimuth, hook height, and jib distance (trolley) were recorded. The gondola was lowered as far as possible without encountering deep understory vegetation, usually to between 5 and 10 m height. Photos were taken under dawn and (or) overcast conditions, which allowed for acquisition of high-quality images in which sky and foliage were well differentiated (Fig. 1). Hook height (distance below the crane jib) was transformed into height above the ground by correcting for ground elevation and the height of the camera within the gondola. Thirty three additional photographs were taken on a regular 25 × 25 m grid at 1.5 m above the forest floor to estimate forest floor conditions beyond the nine gaps.

Photographs were analyzed with the program CANOPY 2.1 (Rich 1989). Because the steel cage of the gondola precluded accurate compass measurements to orient the photos to true north, the azimuth of the crane jib was used for orientation. The CANOPY editor was used to remove the jib, cables, and other components of the crane and gondola. One person (S.B.W.) analyzed all photos.

Standard “site factors” were calculated. Indirect site factor (ISF) is the proportion of sky visible from the photo point, and measures the penetration of diffuse radiation. I assumed a uniform overcast sky (UOC). Direct site factor (DSF) is the proportion of the sunpath not obscured by foliage, weighted by a function of solar elevation angle to account for atmospheric absorption. ISF and DSF were also cosine corrected to a horizontal surface to incorporate insolation data from horizontal sensors (ISFC and DSFC). Analysis included the interactive choice of a threshold gray value to separate canopy from sky. Trees contrasted strongly with overcast sky, so that choosing a threshold during CANOPY analysis was straightforward. Repeat analysis of a subset of 20 photos spanning the whole range of canopy cover showed repeatability (RMS error) of 0.02. The lowest site factors were well within a range

Fig. 1. Example vertical transect of photographs every 5 m height. Height profiles of ISFC and DSFC corresponding to photographs are in the small graph to the right.



(0.03–0.15) where digital analysis techniques provide reliable estimates (Rich 1990).

Site factors were converted into total yearly and monthly insolation. No long-term data were available from WRCCRF itself. Long-term (1961–1990) shortwave insolation, divided into diffuse and direct components, has been measured at Portland, Oreg., about 65 km west of WRCCRF (NREL national solar radiation data base). Portland data capture the overall seasonality and cloud cover of region, but insolation at WRCCRF differs slightly from that in Portland (D. Shaw, personal communication), primarily because Portland experiences coastal fog that penetrates up the Columbia River during the summer, while WRCCRF is beyond the summer fog zone. However, the position of WRCCRF on the windward slope of the Cascade Range also increases cloudiness during the passage of weak summer cold fronts. The advantages of using the long-term Portland data include the division into direct and diffuse insolation and interannual and monthly variation over the 30-year period. The magnitude of the differences between Portland and WRCCRF can be quantified once longer term on-site records become available.

Mean yearly insolation was calculated as a weighted sum of ISFC and DSFC (cosine corrected):

$$[1] \quad S_{\text{tot}} = S_c \times \text{ISFC} + S_b \times \text{DSFC}$$

where S_{tot} , S_d , and S_b are total, diffuse, and direct (beam) insolation, respectively.

Insolation was expressed as a daily average ($\text{MJ}\cdot\text{m}^{-2}\cdot\text{day}^{-1}$) or summed through time for a yearly total. A similar weighting scheme was used for monthly insolation, using monthly DSFC and mean daily direct and diffuse insolation for each month. Because of slight differences in ground elevation from gap to gap, results were averaged for 5-m increments to create “gap-averaged” site factors. The standard deviation and range of site factors and insolation at each height measured intergap variability.

I estimated interannual variability of total yearly direct and indirect insolation for each year from 1961–1990. I also calculated the theoretical maximum global insolation by assuming clear sky conditions year round (Lund 1980). The coefficient of variation ($\text{CV} = \text{SD}/\text{mean}$) at each height was calculated for intergap, interannual, and monthly variability. I also calculated the interannual variability (SD) of monthly insolation by calculating insolation for every month in the 30-year Portland record.

I simulated hourly insolation for the winter solstice, spring equinox, and summer solstice under both clear and cloudy skies. Hourly direct and diffuse clear-sky insolation on a horizontal surface was calculated for each date by standard equations (Lund 1980) assuming an atmospheric transmissivity of 0.8 (very clear). I also calculated hourly diffuse insolation on a horizontal surface under uniform stratocumulus clouds, using equations extracted from List (1971). Stratocumulus clouds provided an intermediate brightness between lower altitude stratus and fog and higher cloud types, and are a common feature of storm systems in the region. Other cloud types could also be simulated by these methods. Hourly unweighted openness along monthly sunpaths was averaged across gaps for each height, and hourly insolation was calculated as

$$[2] \quad S_{\text{tot}} = \text{ISFC} \times S_d + O_b \times S_{bc}$$

where O_b is the hourly openness along the sunpath and S_{bc} is the hourly direct insolation cosine corrected for the horizontal surface. The direct component drops out on cloudy days.

Leaf area index (LAI) is an important structural characteristic of plant canopies, and the vertical distribution of leaves (or needles) affects interrelated canopy functions such as light interception, photosynthesis, and transpiration (Chen et al. 1997). LAI was defined here as the one-sided area of leaves per unit ground area (m^2/m^2). Hemispherical photographs can be used to estimate LAI

by inverting the Beer–Lambert law for the transmission of light through a turbid medium (Chen et al. 1991). I used the program LAICALC (Rich et al. 1995), which solves the equation

$$[3] \quad P(q) = \exp\left(\frac{-G(q)\Omega L_t}{\cos(q)}\right)$$

where $P(q)$ is the gap fraction at the view zenith angle q , and is calculated directly from the hemispherical photograph; $G(q)$ is the projection coefficient characterizing the foliage angle distribution; L_t is the plant area index including foliage and woody areas; and Ω is a parameter determined by the spatial distribution of foliage and other obstructions and is generally known as the “clumping factor”: $\Omega > 1$ when foliage is uniformly distributed, $\Omega = 1$ when foliage is randomly distributed, and $\Omega < 1$ when foliage is clumped. Only the product ΩL_t can be calculated from gap fraction and is referred to as “effective LAI” (L_e). Coniferous forests are highly clumped at multiple scales, which leads to substantial underestimation of L_t by optical methods without consideration of clumping (Chen et al. 1997). Because no direct measure of Ω at WRCCRF was available, a first approximation was estimated by the ratio of L_e from LAICALC to LAI estimated from sapwood area (Easter and Spies 1994) and litter fall (Harmon et al. 1998). I did not correct for bole and branch area or epiphyte load to calculate LAI for the trees alone. Incremental L_e in 5-m classes produced vertical profiles of L_e ; L_e from the forest floor was estimated from the 33 photographs on the 25×25 m grid at 1.5 m height.

Results

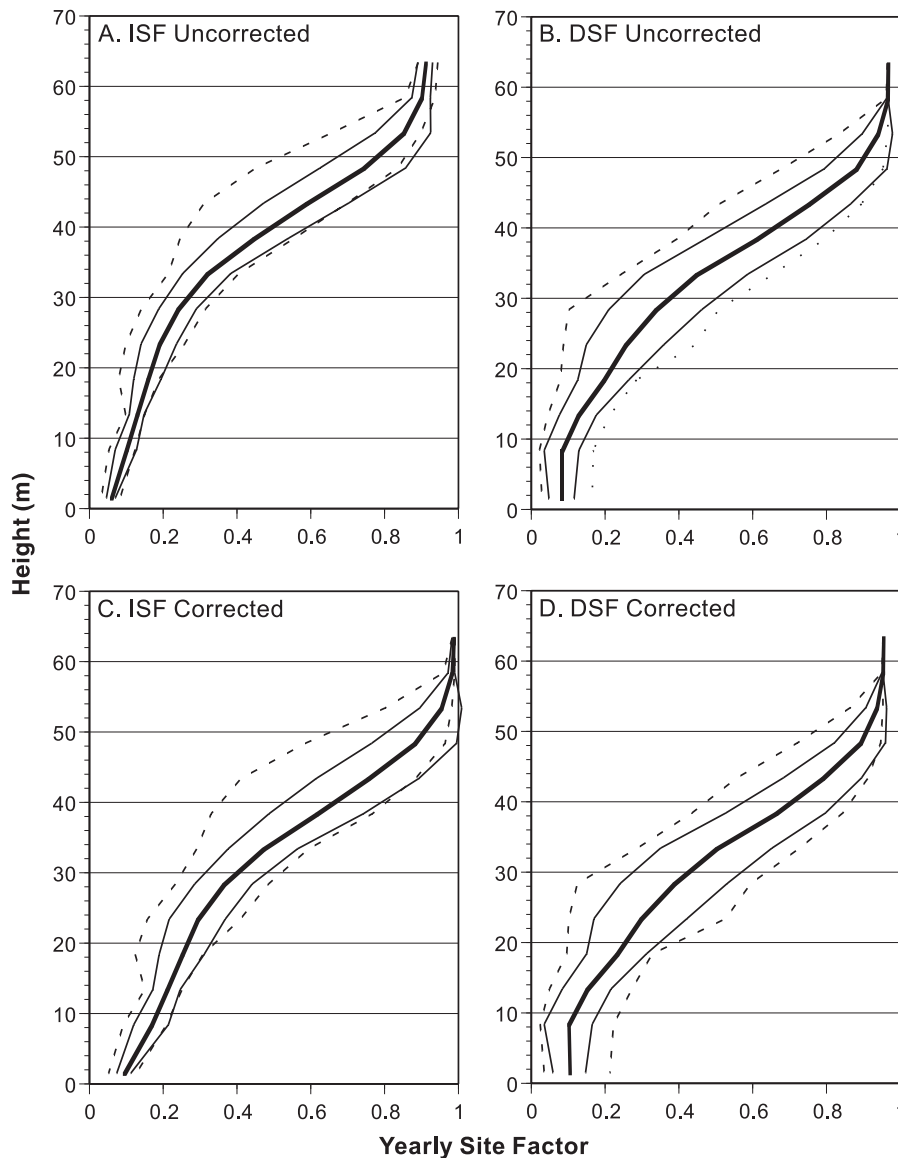
A representative vertical transect showed conditions during descent into a canopy gap (Fig. 1, photographs). At the top of the forest (62–47 m), the only natural obstructions to insolation were the surrounding mountains and a few emergent crowns of the tallest Douglas-firs. During descent, subdominant hemlocks appeared at 42 m (compare the form of the hemlock on the left with the taller Douglas-fir on the right), producing a rapid rate of change in canopy cover from 42 to 22 m. Conditions darkened near the bottom of the gap (7 m), but the porous nature of the forest was apparent. There were substantial open areas at zenith angles $>45^\circ$ (halfway between the center and rim of the photograph), similar to photographs from the forest floor taken by Van Pelt and North (1996).

These changes in appearance were captured quantitatively with ISFC and DSFC (cosine corrected; Fig. 1, graph). From 62 to 47 m both site factors remained near 1, and then rapidly decreased as hemlocks appeared around 42 m. At 22 m, there was another inflection point, and below 22 m, site factors decreased more slowly. This sigmoidal shape was characteristic of most individual transects.

Gap-averaged ISF and DSF exhibited sigmoidal patterns similar to the sample transect (Figs. 2A–2D). Corrected values were always slightly higher than uncorrected values, because in these gaps the overhead areas (more heavily weighted by the cosine correction) were always open. Corrected and uncorrected site factors were highly correlated ($r^2 = 0.99$), and I worked with corrected values for insolation calculations.

Gap-averaged ISFC followed a sigmoidal decrease, with little change above 55 m (>0.95), the most rapid change from 50 to 35 m (0.5), and a lesser rate of change below 35 m to 10 m (0.2) to 0.1 at 1.5 m (Fig. 2C). Mean DSFC

Fig. 2. Height profiles of ISFU, DSFU, ISFC, and DSFC. The thick line is the mean, the inner lines are ± 1 SD, and the outer lines are the range.



showed a similar pattern (Fig. 2D). Intergap variability was minimal at the very top of the canopy, rapidly increased, and remained large at lower heights. The maximum intergap variability in ISFC occurred between 40 and 45 m, and maximum intergap variability in DSFC occurred between 25 and 30 m. Intergap variability in DSFC was generally larger than that of ISFC, especially lower in the canopy.

Direct insolation penetrated deeper into the canopy as solar elevation increased from December through June (Fig. 3). In December, DSFC was 0.50 at 42 m, virtually no direct insolation penetrated below 20 m, and gap-averaged DSFC was strongly sigmoidal. In March, DSFC was 0.50 at 35 m, some direct insolation penetrated to 10 m (DSFC = 0.10), and the sigmoidal shape was still apparent. By May and June, DSFC was 0.50 at 25 m, DSFC at 10 m increased to 0.20, and curves were nearly linear from 50 to 10 m. DSF was symmetrical around the solstice months, so the pattern was mirrored from June to December.

Thirty-year averages of yearly and monthly direct and diffuse insolation on a horizontal collector at Portland clearly showed the seasonal cycle of the Pacific Northwest (Fig. 4). On a yearly basis, global insolation averaged $12.7 \text{ MJ}\cdot\text{m}^{-2}\cdot\text{day}^{-1}$ evenly distributed between direct and diffuse components (49–51%). On a monthly basis, December provided the least insolation, because of low solar elevation and high cloudiness (69% diffuse). July provided the most because of high solar elevation and low cloudiness (39% diffuse). The intensity of diffuse insolation in July (about $9 \text{ MJ}\cdot\text{m}^{-2}\cdot\text{day}^{-1}$) exceeded the above-canopy global insolation for the period October–February. Under completely clear skies, insolation would be symmetrical around the solstices. In actuality, the months after the summer solstice were sunnier than the months preceding it. For example, average daily insolation in April was 56% diffuse, compared with 40% diffuse in August.

Yearly insolation in the gaps exhibited a sigmoidal height

Fig. 3. Height profiles of gap-averaged monthly DSFC. The seasonal progression of direct light penetration into the forest as solar elevation increase can be readily seen.

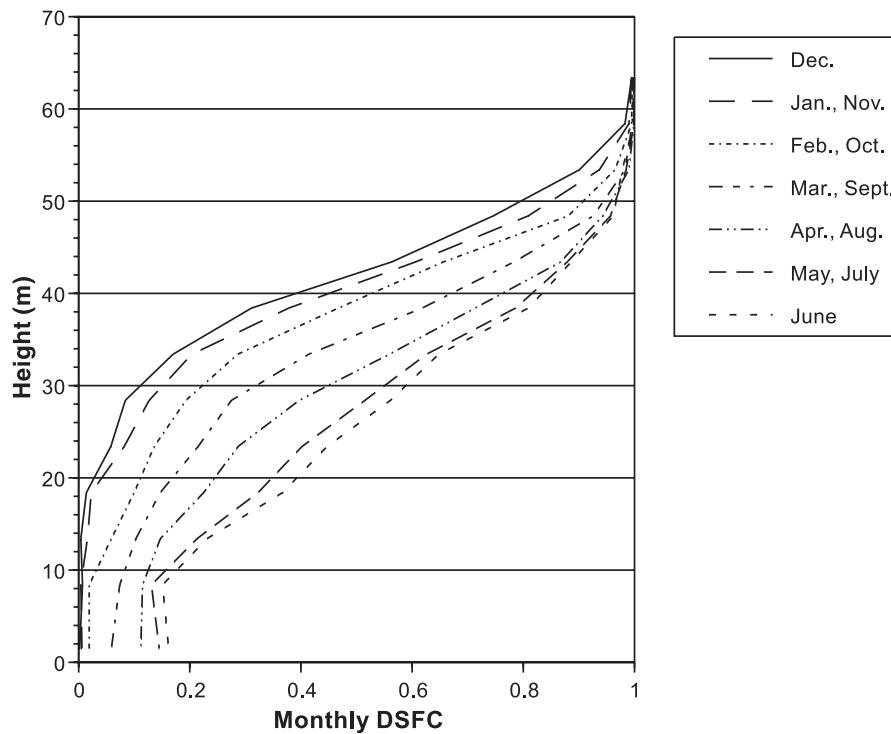
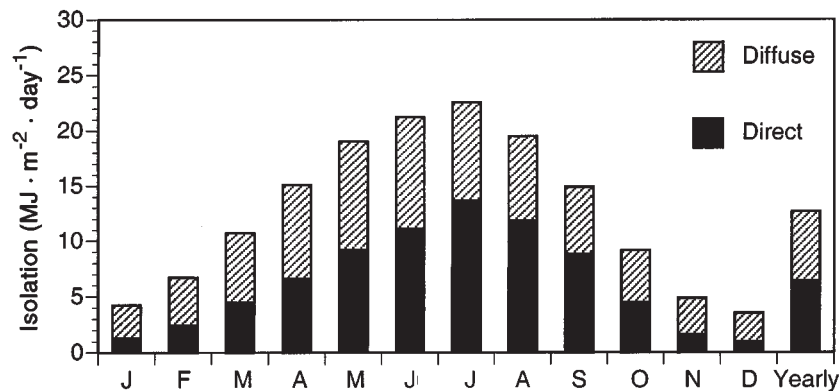


Fig. 4. Daily direct and diffuse insolation by month for Portland, Astoria, and Yakima. Yearly average is the final column.



profile (Fig. 5A). Each curve was nearly equal combination of ISFC and DSFC, according to eq. 1, because of equal weighting of yearly direct and diffuse radiation at Portland (Fig. 4). Above 55 m there was little obstruction and yearly insolation averaged more than 4250 MJ/m². Below 50 m, yearly insolation decreased steadily to 2000 MJ/m² at 30 m, followed by a less rapid decrease to 800 MJ/m² at 10 m, and <500 MJ/m² at 1.5 m. Fifty percent of the yearly insolation was intercepted above 32 m, 80%, above 15 m; and 90%, above the lowest understory (1.5 m). Intergap variability in yearly insolation was large, and absolute differences were greatest between 30 and 40 m (range 1500–2000 MJ/m²).

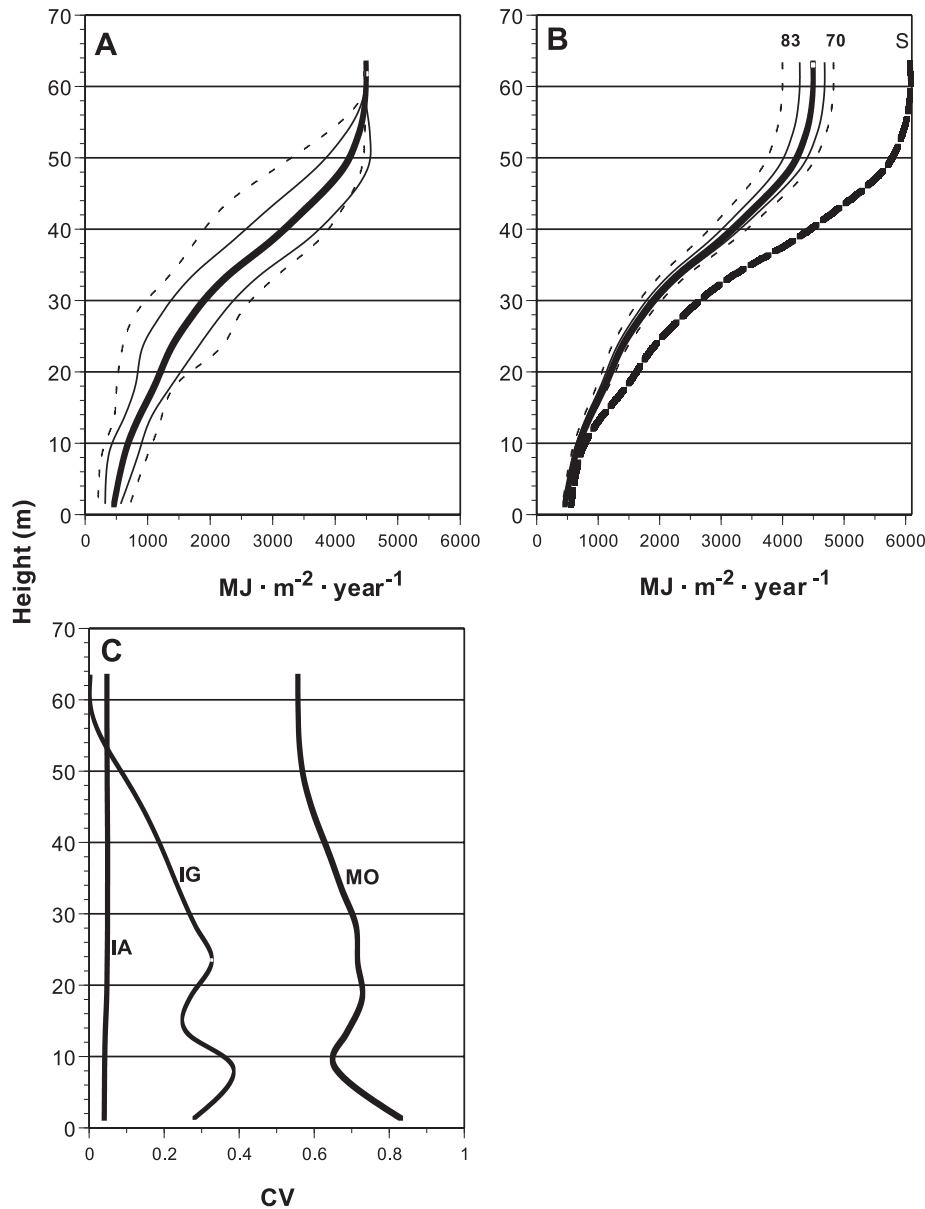
Yearly partitioning between direct and diffuse insolation also changed with height. From 65 to 20 m, 50% of yearly insolation was diffuse, rising to 58% at 15 m and to 62% below 10 m. This pattern of partitioning was a direct result of

the relative values of ISFC and DSFC (Figs. 2C and 2D). From 65 to 20 m, ISFC and DSFC were equal; below 20 m, ISFC was larger than DSFC.

Portland exhibited interannual variation in total insolation (Fig. 5B). At the top of the canopy, the sunniest year (1970) delivered 4827 MJ/m² of which 47% was diffuse, and the cloudiest year (1983) delivered 3997 MJ/m² (53% diffuse). Interannual differences were maintained deep in the canopy but were muted at the lowest heights, with an absolute range of <100 MJ/m² below 10 m. To illustrate the magnitude of cloudiness effects, theoretical clear-sky yearly insolation delivered 6060 MJ/m² at the top of the canopy, of which 15% was sky diffuse, reduced to less than 650 MJ/m² at 1.5 m (Fig. 5B, right-hand curve).

Relative values of intergap and interannual variation were compared using the CV at each height class (Fig. 5C). The

Fig. 5. (A) Height profile of gap-averaged 30-year mean insolation using Portland insolation data. The thick line is the mean, the inner lines are ± 1 SD, and the outer lines are the range. (B) Interannual variation of Portland data. The thick line is the mean, the inner lines are ± 1 SD, and the outer lines are the maximum and minimum (labeled by year). The far right-hand profile is for a completely clear year. (C) Height profile of CV (coefficient of variation, SD/mean) of interannual (IA), intergap (IG), and monthly (MO) insolation.



intergap CV changed with height, linearly increasing from 60 m to a local maximum of 32% at 27 m, decreasing to 25% at 15 m and increasing again to nearly 40% below 10 m. The CV for interannual variation remained below 5% at all heights (Fig. 5D).

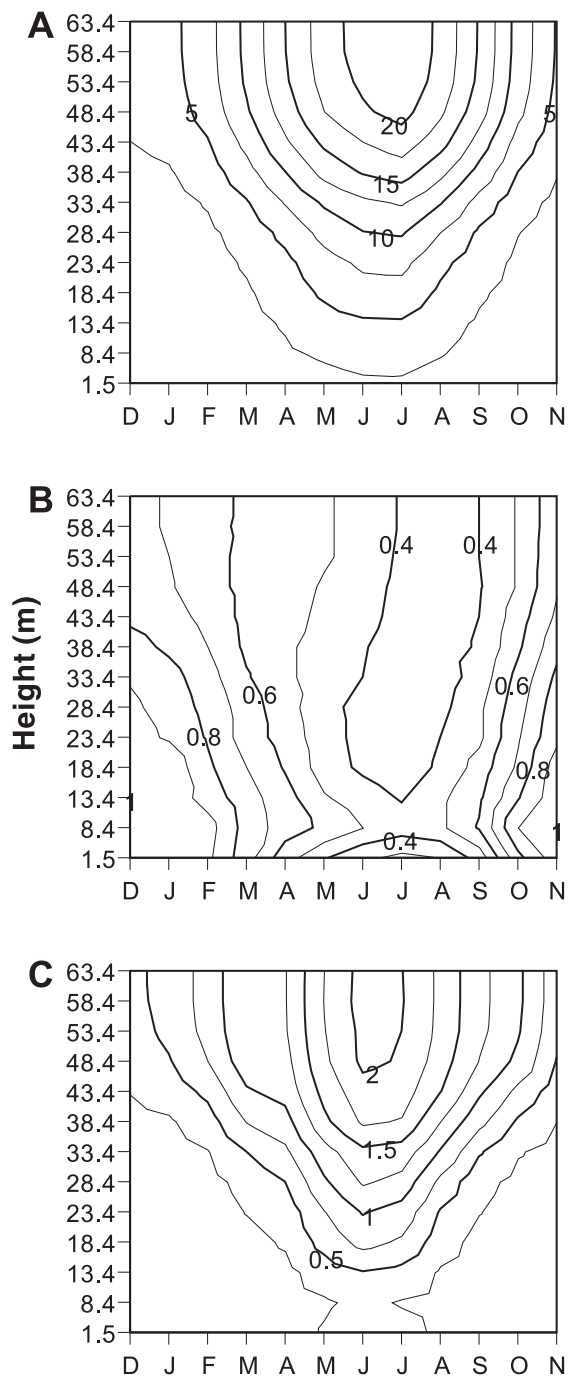
A height–time–energy plot showed strong seasonal variation in the penetration of daily insolation (Fig. 6A). All heights received little daily insolation in the winter months, because of low global insolation. Global insolation increased with solar elevation, as did the depth of direct beam penetration leading to a peak in July. Mean values for the forest floor were never greater than $2.5 \text{ MJ}\cdot\text{m}^{-2}\cdot\text{day}^{-1}$. Yearly curves were asymmetric around the summer solstice because of the cloudiness patterns discussed above (Fig. 4). The sea-

sonal amplitude was greatest in absolute terms higher in the canopy, but relative variation measured by the CV across months was greatest in winter than in summer. The deep understory was dominated by diffuse insolation for much of the year, but in June, July, and August, a substantial proportion of the radiation deep in the forest was direct.

The monthly fraction of diffuse radiation varied with height and month (Fig. 6B). The diffuse fraction increased toward low canopy levels in all months and was greater in winter than in summer. The deep understory was dominated by diffuse insolation for much of the year, but in June, July, and August, a substantial proportion of the radiation deep in the forest was direct.

Interannual variability in average monthly insolation (measured by the SD) appeared to be relatively low, barely exceeded $2 \text{ MJ}\cdot\text{m}^{-2}\cdot\text{day}^{-1}$ in June and July near the top of the

Fig. 6. (A) Height–time profiles of monthly mean daily insolation ($\text{MJ}\cdot\text{m}^{-2}\cdot\text{day}^{-1}$) for Portland. (B) Proportion of diffuse insolation by height and month through the year. (C) Interannual variation (SD) of monthly insolation by height and month for 1961–1990 Portland data.



canopy, and becoming greatly muted deeper in the canopy and in winter months. However, in relative terms as measured by the CV, interannual variability at the monthly scale was on the order of 10%, about twice that exhibited on a yearly basis.

The hourly distribution of clear-sky and cloudy-day insolation on the winter solstice, spring equinox, and summer solstice showed unimodal shapes, beginning at sunrise, peaking

at noon, and ending at sunset (Figs. 7A, 7B, and 7C). Seasonal variation was strong. In December under clear skies, global insolation was low, peaking at $0.63 \text{ MJ}\cdot\text{m}^{-2}\cdot\text{h}^{-1}$ at noon. On the cloudy day, insolation peaked at $0.33 \text{ MJ}\cdot\text{m}^{-2}\cdot\text{h}^{-1}$ at noon. In March, insolation peaked at $2.4 \text{ MJ}\cdot\text{m}^{-2}\cdot\text{h}^{-1}$ and $0.95 \text{ MJ}\cdot\text{m}^{-2}\cdot\text{h}^{-1}$ at noon on the clear and cloudy days, respectively, and insolation penetrated deeper into the forest. In June, insolation peaked at $3.3 \text{ MJ}\cdot\text{m}^{-2}\cdot\text{h}^{-1}$ and $1.3 \text{ MJ}\cdot\text{m}^{-2}\cdot\text{h}^{-1}$ at noon on the clear and cloudy days, respectively. Average peak insolation at the forest floor in June never reached $1 \text{ MJ}\cdot\text{m}^{-2}\cdot\text{h}^{-1}$ on the clear day.

In December, penetration into the forest on the clear day was minimal because of low solar elevations. The seasonal increase of insolation was driven by higher solar elevations that increased the depth of direct penetration and provided higher hourly global insolation. The seasonal changes of insolation with height on cloudy days were a strict function of global hourly insolation, as ISFC was assumed to not change through the year.

The jaggedness in clear-day contours contrasts with the smoothness in cloudy-day contours, and the differences were driven by high variation in canopy cover at half-hour intervals along narrow sunpaths. A single branch can effectively cover a half-hour increment along monthly sunpaths, so only nine samples at any given height leads to high spatial variability at that fine temporal scale.

One-sided L_e estimated by LAICALC from the 33 forest floor photographs was $3.7 \pm 0.6 \text{ m}^2/\text{m}^2$ (mean \pm SD, range 2.7–5.0). The vertical cumulative profile (Fig. 8A) showed 50% of total L_e below 20–25 m and only 13.5% above 40 m. Incremental L_e increased slowly from 60 to 50 m, followed by more rapid linear increase from 50 m to a local peak at 30–35 m, a local minimum around 20 m, and another local maximum around 5–10 m (Fig. 8B). Structurally, the canopy above 50 m was dominated by emergent Douglas-fir, and the 30- to 35-m peak corresponded to the hemlock middle story. The relatively open area between 25 and 15 m was below the lower live branches of these hemlocks. The 5- to 10-m peak corresponded to *Acer* and shade-tolerant conifers such as yew and young hemlocks.

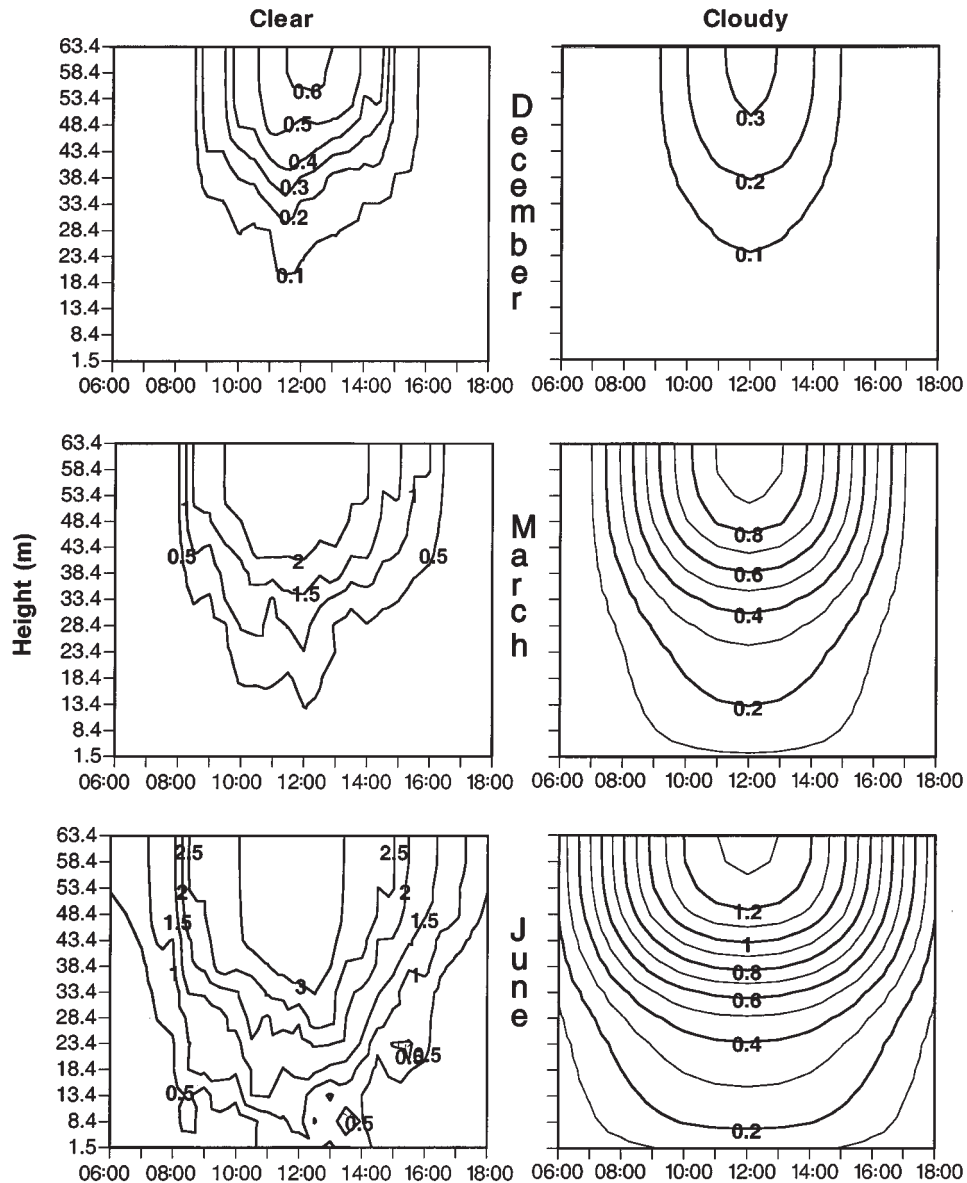
The mean “leaf” angle estimated by LAICALC was $57 \pm 1^\circ$ and did not change with height. Given the resolution of the photographs, the angle likely measures shoot and branch orientation, as opposed to individual needles.

Discussion

The combination of the canopy crane, hemispherical photography, and long-term insolation data provided the means to effectively explore spatial and temporal components of insolation variability in this forest. In contrast with other studies of forest light environments, I was able to characterize vertical distribution, elements of horizontal distribution at various heights, and temporal distribution through the year and through select days as it varies with height. The long-term insolation data from Portland provided the means to estimate absolute amounts of insolation, fractions of direct and diffuse insolation, and the effects of varying cloudiness from interannual variation.

The major potential bias in these results is that the estimates above 1.5 m were for the centre of canopy gaps,

Fig. 7. Height–time profiles of half-hourly insolation ($\text{MJ}\cdot\text{m}^{-2}\cdot\text{h}^{-1}$) for clear and cloudy days for December, March, and June.



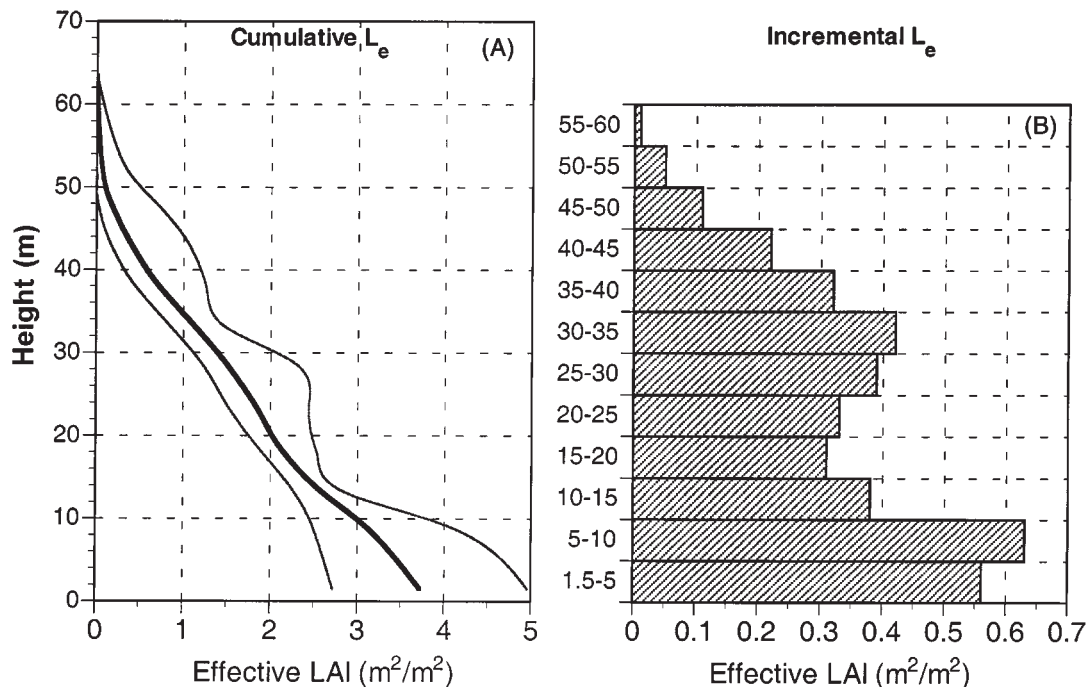
which were some of the best-lit portions of the forest and represent the active canopy layer where most photosynthesis and evapotranspiration occurs. Live foliage was generally concentrated on the outer 1–2 m of branches, and volumes within tree crowns were virtually empty except for branches. Sampling within the tree crowns at various heights (not possible with current crane access) could provide a somewhat different view of the vertical insolation gradient and would greatly increase the degree of horizontal variability at any given height.

The 1.5-m samples were distributed across a wide range of canopy conditions, which may account for the behavior of DSF and monthly diffuse fractions estimated for the forest floor. DSF at 8.4 m was the same as DSF at 1.5 m on a monthly and yearly basis. (Figs. 2B, 2D, and 3). DSF usually would be highest well north of gap centers (Canham et al. 1990; Van Pelt and North 1996); if the 1.5-m height were sampled at the bottom of gaps, then one might expect to see

a continual decrease of DSF to the forest floor. The absolute differences in insolation this bias produced, however, may be relatively small because of the low insolation at ground level.

I sampled only one component of horizontal variability: intergap variability. Each gap had a unique vertical profile that reflected the heterogeneity of the forest, and differences between gaps led to annual differences of up to $2000 \text{ MJ}\cdot\text{m}^{-2}\cdot\text{year}^{-1}$ at the same height. Variation within gaps (intragap variation) keeping height constant may be substantial in a north–south direction, as the north side of a gap will receive more direct sun than the south side (Van Pelt and North 1996). At ground level, such north–south differences appear to be muted in old-growth Douglas-fir – western hemlock forests because of the dense middle story of hemlocks (Canham et al. 1990). Higher in the canopy, though, north–south variation may be substantial. Data from a study on dwarf mistletoe (Shaw and Weiss 2000) suggests that

Fig. 8. Height profiles of (A) Cumulative effective leaf area (L_e) and (B) incremental L_e in 5-m height classes.



yearly insolation may vary from north to south in a gap by a factor of two at heights between 20 and 40 m. However, more systematic evaluation of intragap horizontal variability with height and sampling within tree crowns would greatly enhance the picture of horizontal variability.

Temporal variability occurred at interannual, monthly, and hourly time scales. Interannual variation was a function of cloudiness and produced an above-canopy range of about $900 \text{ MJ}\cdot\text{m}^{-2}\cdot\text{year}^{-1}$ at Portland that became muted in absolute terms deeper in the forest. However, relative interannual variation as measured by the CV was the lowest of all sources of temporal variability (Fig. 4). Monthly variation was a function of both solar angle and cloudiness, and the effect of solar angle was very large as expected at high latitude sites. Cloudiness drove asymmetry around the summer solstice in both total insolation and fraction of diffuse insolation. The model of hourly variation highlighted the peak hourly insolation and the duration and depth of penetration under sun and clouds on different days. The extreme spatial variability of hourly insolation was also apparent by the jagged contours on the clear days compared with the smooth contours on the cloudy days.

Leaf area index has proven to be difficult to measure with non-destructive optical techniques (White et al. 1997). My total LAI estimates ($L_e = 3.7$) were definitely low for this forest type. Measurements of LAI by leaf fall ($9.2 \text{ m}^2/\text{m}^2$, Harmon et al. 1998), and by sapwood area ($9.12 \text{ m}^2/\text{m}^2$; Easter and Spies 1994) were in close agreement. At first approximation, the difference could be attributed to the clumping factor Ω , which greatly affects the interception of insolation relative to absolute LAI. Ω was estimated at 0.4 ($\Omega = L_e/\text{LAI}$ according to eq. 2), indicating a high degree of clumping at WRCCRF. Conifer foliage shows clumping at many scales: needles on shoots, shoots on whorls, whorls on branches, whole tree crowns, and clumps of trees within the

stand. Clumping also differs among species, with the extreme example of flat *Acer* leaves that are held nearly horizontal compared with conifer needles. My estimate of Ω was far lower than that from black spruce (*Picea mariana* (Mill.) BSP) forests ($\Omega = 0.7$, Chen et al. 1997). However, Smith et al. (1993) reported a similar Ω (0.38) for Douglas-fir forests. The complex multistoried and clumped structure of this old-growth forest allowed for substantial light penetration deep within the forest, while at the same time supporting a very large LAI. More work clearly needs to be done to understand clumping patterns of foliage within this forest.

The vertical distribution of effective LAI (L_e) showed a maximum at around 30–35 m and again from 5–10 m. Parker (1997) found maximum L_e at 18 m, but that result is likely caused by the high solar angles in his study. The peak at 30–35 m is consistent with the foliage profile described by Easter and Spies (1994). The gap bias may have influenced this profile and the overall L_e values, but the bias may not be large because areas away from the open zenith in gaps are more heavily weighted by LAICALC because of the $\cos(q)$ term in the denominator of eq. 3. In addition, L_e from the non-gap-biased samples at 1.5 m ($3.7 \text{ m}^2/\text{m}^2$) was not much greater than L_e at 8.4 m ($3.15 \text{ m}^2/\text{m}^2$).

An essential feature of the insolation environment in this forest was the importance of diffuse insolation. Diffuse insolation is qualitatively different from direct beam insolation, and these differences affect both its mode of penetration through the canopy, and its effect on plants when it is intercepted. Because diffuse insolation comes from all sky directions, it provides a more even illumination of the forest, although it can be quite variable from gap to gap (Figs. 2A and 2C). The geometry of light interception by conifer shoots and branches is very different under diffuse than direct insolation (Stenberg et al. 1995), and conifer needles

under even illumination by diffuse insolation may have high photosynthetic efficiency without experiencing heat, water, and light stress that intense direct insolation can produce (Teskey et al. 1995). In addition, evaporative demand is much lower under cloudy conditions, so that stomata may remain open longer through the day. Several conifer stands have shown greater CO₂ uptake rates under diffuse light than under equivalent direct light intensities (Price and Black 1990; Hollinger et al. 1994; Goulden et al. 1997), and models have simulated this effect for whole canopies (Oker-Bloom 1985; Jarvis et al. 1985). Light response curves at the shoot level under diffuse conditions are poorly characterized (B. Bond, personal communication), but physiological measurements under diffuse insolation would be important in understanding stand-level photosynthesis and the high productivity of Pacific Northwest conifer forests. The hourly contours for the cloudy days (Fig. 7) show that substantial diffuse light reaches deep into the forest in March and June, providing even illumination through much of the day that is well above the light compensation point for the major tree species (around 0.04 MJ·m⁻²·h⁻¹; Bond et al. 1999). Under clear skies in June, much of the upper canopy is well above the 90% light saturation point for Douglas-fir and hemlock (0.89 and 0.68 MJ·m⁻²·h⁻¹, respectively; Bond et al. 1999). Light and heat stress may limit photosynthesis at these heights during clear periods. Under cloudy conditions in June, much of the canopy is illuminated at levels that can allow for high photosynthetic rates.

Cloudier conditions in spring occur when the soil is saturated from snowmelt and spring rains, while sunnier conditions in summer coincide with the period of water deficit in this forest. This annual cycle of water excess in winter and spring and deficit in summer is a major constraint on many forest processes (Waring and Franklin 1979). Estimates of evaporative demand from these insolation profiles and climatic data may shed light on patterns of seasonal and interannual water stress in coniferous forests, such as where in the canopy maximal transpiration occurs as a function of insolation and leaf area.

The forest canopy not only shapes the insolation environment but also responds to it in several ways. Tree and branch growth may increase in high insolation regions of the canopy, and conversely, needles and branches are shed in low insolation regions where they cannot maintain a positive carbon balance (Margolis et al. 1995). Vertical insolation gradients greatly affect photosynthetic capacity and realized assimilation rates within and among trees (Holbrook and Lund 1995). Both Douglas-fir and western hemlock trees exhibit gradients of greater needle mass and nitrogen content with higher insolation, which can increase photosynthetic capacity of the whole canopy (Bond et al. 1999). Conversely, these needle morphologies may themselves be a strong indicator of average insolation levels at various positions in the canopy. Understanding how these patterns affect the photosynthetic capacity of the whole canopy through the year would involve linking the monthly insolation contours (Fig. 6) or hourly contours (Fig. 7) with models that consider photosynthetic capacity under direct and diffuse light and water stress as well as the vertical distribution of leaf area. Because of the nonlinear response of CO₂ assimilation to light levels and other environmental factors (Stenberg et

al. 1995; Bond et al. 1999), simple averaging over time and space may not be appropriate for estimating canopy-level assimilation.

The crane provided unique opportunities to paint a picture of spatial and temporal variation of insolation in this particular forest. Transporting the results to other forests of the Pacific Northwest poses challenges. Insolation data exist for many other stations in the Pacific Northwest (NREL 1999). Douglas-fir – western hemlock forests extend across more than 10° of latitude, but structural differences among forests on different soil types, across latitude, among microclimates, and with different species composition provide additional axes of variability. On a global scale, similar sampling at the six other canopy cranes in the world would provide contrasts among biomes with far different sunpaths, cloudiness, and forest structure.

Insolation has pervasive effects on the structure and function of forest ecosystems. Because this study provides a detailed description of the spatial and temporal structure of insolation in a tall forest, it is of broad interest to forest ecologists. On a regional level, WRCCRF has become a focal point for integrated studies of forest structure and function in relation to global change (Suchanek 1997). This study provides key baseline data for relating insolation to numerous facets of forest ecology, including photosynthesis, water balance, allocation and cycling of carbon and nutrients, distribution of epiphytes (McCune et al. 1997), insects (Shaw 1998), and mistletoes (Shaw and Weiss 2000) among other studies at WRCCRF.

Acknowledgments

D. Shaw provided crane access and field expenses at WRCCRF. M. Creighton artfully maneuvered the crane into position. G. Parker provided coordinates for gaps. P. Rich ran the LAICALC program and provided ongoing technical advice on hemispherical photography. Two anonymous reviewers and J. Volney provided comments that improved the manuscript. Support for the author was provided by P. and H. Bing.

References

- Becker, P., and Smith, A.P. 1990. Spatial autocorrelation of solar radiation in a tropical moist forest understory. *Agric. For. Meteorol.* **52**: 373–379.
- Canham, C.D., Denslow, J.S., Platt, W.J., Runkle, J.R., Spies, T.A., and White, P.S. 1990. Light regimes beneath closed canopies and tree-fall gaps in temperate and tropical forests. *Can. J. For. Res.* **20**: 620–631.
- Chen, J.M., Black, T.A., and Adams, R.S. 1991. Evaluation of hemispherical photography for determining plant area index and geometry of a forest stand. *Agric. For. Meteorol.* **56**: 129–143.
- Chen, J.M., Rich, P.M., Gower, S.T., Norman, J.M., and Plummer, S. 1997. Leaf area index of boreal forests: theory, techniques, and measurements. *J. Geophys. Res.* **102**: 29 429 – 29 443.
- Clark, D.B., Clark, D.A., Rich, P.M., Weiss, S.B., and Oberbauer, S.F. 1996. Landscape-scale analysis of forest structure and understory light environments in a neotropical lowland rain forest. *Can. J. For. Res.* **26**: 747–757.
- Easter, M.J., and Spies, T.A. 1994. Using hemispherical photography for estimating photosynthetic photon flux density under

- canopies and in gaps in Douglas-fir forests of the Pacific Northwest. *Can. J. For. Res.* **24**: 2050–2058.
- Geiger, R. 1965. The climate near the ground. Harvard University Press, Cambridge, Mass.
- Gendron, F., Messier, C., and Comeau, P.G. 1998. Comparison of various methods for estimating the mean growing season percent photosynthetic photon flux density in forests. *Agric. For. Meteorol.* **92**: 55–70.
- Goulden, M.L., Daube, B.C., Fan, S.-M., Sutton, D.J., Bazzaz, F.A., Munger, J.W., and Wofesy, S.C. 1997. Physiological response of a black spruce forest to weather. *J. Geophys. Res.* **102**: 28 987 – 28 996.
- Harmon, M.E., Bible, K., Shaw, D., Remillard, S., Sexton, J., Fasth, B., Priestley, A., Chen, J., and Franklin, J.F. 1998. Permanent plots surrounding the Wind River Canopy Crane. Permanent plots of the Pacific Northwest. Forest Sciences Laboratory, Oregon State University, Corvallis. Rep. 1 <<http://www.fsl.orst.edu/lter/pubs/spclrpts/permplot.htm>>
- Holbrook, N.M., and Lund, C.P. 1995. Photosynthesis in forest canopies. *In* Forest canopies. Edited by M.D. Lowman and N.M. Nadkarni. Academic Press, New York. pp. 411–427.
- Holden, C. 1995. Canopy open for business. *Science* (Washington, D.C.), **268**: 645–647.
- Hollinger, D.Y., Kelliher, F.M., Byers, J.M., Hunt, J.E., McSeveny, T.M., and Wier, P.W. 1994. Carbon dioxide exchange between and undisturbed old-growth temperate forest and the atmosphere. *Ecology*, **75**: 134–150.
- Jarvis, P.G., Miranda, H.S., and Muetzelfeldt, R.I. 1985. Modelling canopy exchanges of water vapor and carbon dioxide in coniferous forest plantations. *In* The forest–atmosphere interaction. Edited by B.A. Hutchinson and B.B. Hicks. Reichal, Dordrecht, the Netherlands. pp. 521–543.
- Lerdau, M.T., Holbrook, N.M., Mooney, H.A., Rich, P.M., and Whitbeck, J.L. 1992. Seasonal patterns of acid fluctuations and resource storage in the arborescent cactus *Opuntia excelsa* in relation to light availability and size. *Oecologia*, **92**: 166–171.
- List, F. 1971. Smithsonian meteorological tables. 6th ed. Smithsonian Institution Press, Washington, D.C.
- Lund, P.J. 1980. Solar thermal engineering. John Wiley and Sons, New York.
- Margolis, H., Oren, R., Whitehead, D., and Kaufmann, M.R. 1995. Leaf area dynamics of conifer forests. *In* Ecophysiology of coniferous forests. Edited by W.K. Smith and T.M. Hinckley. Academic Press, San Diego, Calif. pp. 181–216.
- McCune, B., Amsberre, K.A., Camacho, F.J., Clery, S., Cole, C., Emerson, C., Felder G., et al. 1997. Vertical profiles of epiphytes in Pacific Northwest old growth forest. *Northwest Sci.* **71**: 145–152.
- Moffett, M.W., and Lowman, W.D. 1995. Canopy access techniques. *In* Forest canopies. Edited by M.D. Lowman and N.M. Nadkarni. Academic Press, New York. pp. 3–25.
- National Renewable Energy Laboratory (NREL). 1999. National solar radiation data base. <http://rredc.nrel.gov/solar/old_data/nsrdb/>
- Nicotra, A.B., Chazdon, R.L., and Iriate, S.V.B. 1999. Spatial heterogeneity of light and woody seedling regeneration in tropical wet forests. *Ecology*, **80**: 1908–1926.
- Oker-Bloom, P. 1985. Photosynthesis of a Scots pine shoot: simulation of the irradiance distribution and photosynthesis of a shoot in different radiation fields. *Agric. For. Meteorol.* **34**: 32–40.
- Parker, G.G. 1995. Structure and microclimate of forest canopies. *In* Forest canopies. Edited by M.D. Lowman and N.M. Nadkarni. Academic Press, New York. pp. 73–106.
- Parker, G.G. 1997. Canopy structure and light environment of an old-growth Douglas-fir/western hemlock forest. *Northwest Sci.* **71**: 261–270.
- Price, D.T., and Black, T.A. 1990. Effects of short-term variation in weather on diurnal canopy CO₂ flux and evapotranspiration of a juvenile Douglas-fir stand. *Agric. For. Meteorol.* **50**: 139–159.
- Reifsnyder, W.E., Furnival, G.M., and Horowitz, J.L. 1972. Spatial and temporal distribution of solar radiation beneath forest canopies. *Agric. Meteorol.* **9**: 21–37.
- Rich, P.M. 1989. Manual for analysis of hemispherical canopy photography. Los Alamos National Laboratory, Los Alamos, N.M. Rep. LA-11733-M.
- Rich, P.M. 1990. Characterizing plant canopies with hemispherical photographs. *Remote Sens. Rev.* **5**: 13–29.
- Rich, P.M., Clark, D.B., Clark, D.A., and Oberbauer, S.F. 1993. Long-term study of solar radiation regimes in a tropical wet forest using quantum sensors and hemispherical photography. *Agric. For. Meteorol.* **65**: 107–127.
- Rich, P.M., Chen, J., Sulatycki, S.J., Vashisht, R., and Wachspress, W.S. 1995. Calculation of leaf area index and other canopy indices from gap fraction: a manual for the LAICALC software. Open File Report. Kansas Applied Remote Sensing Program, Manhattan.
- Shaw, D.C. 1998. Distribution of larval colonies of *Lophocapa argenta* Packard, the silver spotted tiger moth (Lepidoptera: Arctiidae), in an old growth Douglas fir/western hemlock forest canopy, Cascade Mountains, Washington State, USA. *Can. Field Nat.* **112**: 250–253.
- Shaw, D.C., and Weiss, S.B. 2000. The association of light environment and the occurrence of aerial shoots in hemlock dwarf mistletoe. *Northwest Sci.* **74**: 306–315.
- Smith, N.J., Chen, J.M., and Black, T.A. 1993. Effects of clumping on estimates of stand leaf area index using the LI-COR LAI-2000. *Can. J. For. Res.* **23**: 1940–1943.
- Stenberg, P., DeLucia, E.H., Schoettle, A.W., and Smolander, H. 1995. Photosynthetic light capture and processing from cell to canopy. *In* Resource physiology of conifers: acquisition, allocation, and utilization. Edited by W.K. Smith and T.M. Hinckley. Academic Press, San Diego, Calif. pp. 3–38.
- Suchanek, T. 1997. Integrated ecosystem studies at the Wind River Canopy Crane Research Facility. University of California, Davis. <<http://nigec.ucdavis.edu/westgec/news/article1.html>>
- Teskey, R.O., Sheriff, D.W., Hollinger, D.Y., and Thomas, R.B. 1995. External and internal factors regulating photosynthesis. *In* Resource physiology of conifers: acquisition, allocation, and utilization. Edited by W.K. Smith and T.M. Hinckley. Academic Press, San Diego, Calif. pp. 105–140.
- Thrichon, V., Walter, J.N., and Laumonier, Y. 1998. Identifying spatial patterns in the tropical rainforest structure using hemispherical photographs. *Plant Ecol.* **137**: 227–244.
- Van Pelt, R., and North, M.P. 1996. Analyzing canopy structure in Pacific Northwest old growth forests with a stand-scale crown model. *Northwest Sci.* **70**(Spec. Issue):15–30.
- Waring, R.H., Franklin, J.F. 1979. Evergreen forests of the Pacific Northwest. *Science* (Washington, D.C.), **204**: 1380–1386.
- White, J.D., Running, S.W., Nemani, R., Keane, R.E., and Ryan, K.C. 1997. Measurement and remote sensing of LAI in Rocky Mountain montane ecosystems. *Can. J. For. Res.* **27**: 1714–1727.
- Whitmore, T.C., Brown, N.D., Swaine, M.D., Kennedy, D., Goodwin-Baily, C.I., and Gong, W.K. 1993. Use of hemispherical photographs in forest ecology: measurement of gap size and radiation totals in a Bornean tropical rain forest. *J. Trop. Ecol.* **9**: 131–151.